

# Supporting Information: Rutile ( $\beta$ -)MnO<sub>2</sub> Surfaces and Vacancy Formation for High Electrochemical and Catalytic Performance

David A. Tompsett,\* Stephen C. Parker, and M. Saiful Islam\*

*Department of Chemistry, University of Bath, Bath BA2 7AY, UK.*

E-mail: dt331@bath.ac.uk; m.s.islam@bath.ac.uk

Phone: +44(0)1225 386521. Fax: +44(0)1225 386231

## Surface Energies of Rutile $\beta$ -MnO<sub>2</sub> from Interatomic Potentials

This study employs well-established interatomic potentials methods, which are reviewed in detail elsewhere.<sup>1,2</sup> The model due to Parker and co-workers<sup>3,4</sup> is employed. The interactions between ions are represented in terms of a long-range Coulmbic term with the addition of an analytic term representing short-range interactions such as chemical bonding. In the model employed these short-range effects are modeled by a Buckingham potential with the form:

$$V_{ij}(r_{ij}) = A \exp(-r_{ij}/\rho) - C/r_{ij}^6 \quad (1)$$

where  $r$  is the interatomic separation and  $A$ ,  $\rho$ , and  $C$  are ion-ion potential parameters. The charges on the Mn and O ions are represented by a rigid ion model, with partial charges. The potential parameters are presented in Table S1. This model reproduces the lattice parameters of rutile MnO<sub>2</sub>

---

\*To whom correspondence should be addressed

within 2% of experiment. In this work we use this accurate interatomic potential model to calculate the surface energies using METADISE up to high indexes. The calculated surface energies are shown in Table S2. The resulting equilibrium crystal morphology from a Wulff construction is shown in Figure S1.

Table S1: Parameters describing the interatomic potentials between component ions of  $\beta$ -MnO<sub>2</sub>.

interaction	A (Å)	$\rho$ (Å)	C (eV/Å <sup>-6</sup> )	species	q(e)
Mn <sup>2.2+</sup> -Mn <sup>2.2+</sup>	23530.50	0.156	16.00	Mn <sup>2.2+</sup>	2.20
Mn <sup>2.2+</sup> -O <sup>1.1-</sup>	15538.20	0.195	22.00		
O <sup>1.1-</sup> -O <sup>1.1-</sup>	11782.76	0.234	30.22	O <sup>1.1-</sup>	-1.10

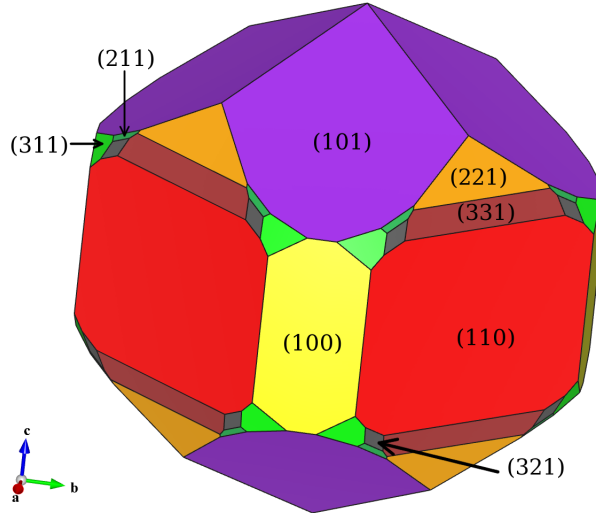


Figure S1: Predicted morphology of  $\beta$ -MnO<sub>2</sub> from interatomic potentials.

## Methodology in the PBE+U Framework

The electronic ground state of rutile MnO<sub>2</sub> possesses a low temperature magnetic transition to anti-ferromagnetic order at  $T = 92$  K.<sup>5</sup> Below this temperature transport measurements show a growing resistivity that reaches  $\sim 10^5$   $\Omega$  cm at  $T = 0$  K, which indicates insulating behavior.<sup>6</sup> Early studies by Franchini *et al.*<sup>7</sup> applying PBE+U to this material in the spherically averaged Dudarev implementation,<sup>8</sup> however, predicted a ferromagnetically ordered metal in contravention of experiment.

Yet a recent study by some of the present authors<sup>9</sup> showed that application of PBE+U in the fully-localized limit<sup>10</sup> gave a good reproduction of both the low temperature magnetic order and band gap. The reader is referred to that work for a detailed discussion. Consequently, the fully-localized limit has been applied throughout the present work.

An important aspect in the use of PBE+U is the selection of an appropriate  $U$  value for the system. This may be achieved for a given material within the framework of Density Functional Theory (DFT) by a self-consistent calculation.<sup>11</sup> In the present work an additional complication is introduced due to the desire to study oxygen vacancy formation at surfaces, which results in a change of oxidation state of the transition metal from  $\text{Mn}^{4+}$  to  $\text{Mn}^{3+}$ . Therefore, a value of  $U$  must be chosen to represent the system in both states. To achieve this we have followed the practice in previous DFT+U works involving changes in oxidation state, for instance for Li-ion intercalation,<sup>12</sup> by calculating the value of  $U$  in both oxidation states and then utilizing the average between the two. It is important to note that the self-consistent calculation of  $U$  is employed to calculate the spherical part of the PBE+U interaction, which in the framework of fully-localized limit is appropriately expressed as  $(U - J)$ ,<sup>10</sup> which we do from here on. In this work we choose a value of  $(U - J) = 5.1$  eV, which is the average of the self-consistently calculated values for  $\text{Mn}^{4+}$  ( $(U - J) = 5.5$  eV) and  $\text{Mn}^{3+}$  ( $(U - J) = 4.7$  eV). The  $\text{Mn}^{3+}$  calculation was performed using  $\beta$ -LiMnO<sub>2</sub>, which retains the same structural features as  $\beta$ -MnO<sub>2</sub> with a differing oxidation state for Mn. Since the Slater integrals  $F^2$  and  $F^4$  (that determine exchange and the anisotropy of the Coulomb interaction) are typically weakly screened in solids<sup>13,14</sup> we employ an atomic-limit value of  $J = 1.0$  eV, which is appropriate to  $\text{Mn}^{4+}$  and  $\text{Mn}^{3+}$ .

## Reconstruction of the (111) Surface

The (111) surface, which with its calculated surface energy of  $1.42 \text{ Jm}^{-2}$ , is very near to being expressed in the morphology. Lowering the surface energy by just  $0.02 \text{ Jm}^{-2}$  brings the (111) surface into the Wulff morphology. However, the low energy of  $1.42 \text{ Jm}^{-2}$  is only obtained if the surface

is subjected to a simple reconstruction to improve its Mn-O coordination as shown in Fig. S2. This raises an interesting case where a simple surface reconstruction lowers the energy significantly. The surface that is cleaved from the bulk crystal, shown in Fig. S2(a), possesses a 3-fold and a six-fold coordinate surface Mn and results in a surface energy of  $2.06 \text{ Jm}^{-2}$ . If the surface is reconstructed by a simple movement of an outer oxygen, as indicated by the dotted line in Fig. S2(a), from the 6-fold site to the 3-fold site we obtain the reconstructed surface shown in Fig. S2(b). This reconstructed surface possesses 5-fold coordinate and 4-fold coordinate manganese ions and after relaxation possesses a surface energy of  $1.42 \text{ Jm}^{-2}$ . The substantial reduction in surface energy afforded by this reconstruction clearly indicates the importance of surface Mn coordination.

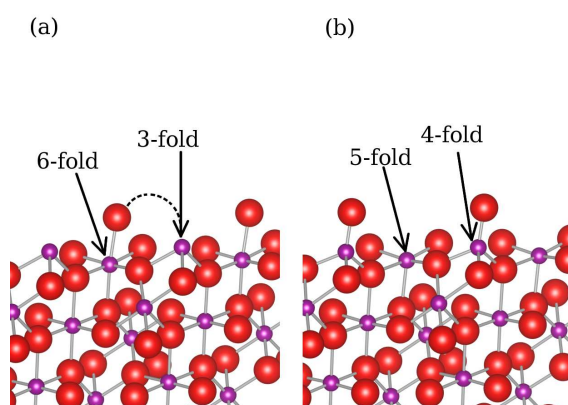


Figure S2: Structure of the (111) surface of  $\beta\text{-MnO}_2$ : (a) Before reconstruction and (b) after reconstruction. The dashed line indicates the simple movement of the oxygen ion that reduces the surface energy.

## Oxygen Vacancies at Rutile $\beta\text{-MnO}_2$ Surfaces from PBE+U

In this work we are interested in oxygen vacancy formation with reference to catalytic processes. These processes are likely to occur at isolated sites on the surface and therefore the dilute limit formation energy for oxygen vacancies is a relevant quantity. The formation energy of oxygen vacancies at surfaces has been converged with respect to our slab calculation geometry. In Figure S3 the convergence of the formation energy with respect to the separation of the defect from its nearest periodic image in the surface plane is shown. Clearly for separations  $> 15 \text{ \AA}$  the defect

energy is converged to within an error of 0.02 eV. In addition Figure S4 shows the convergence of the formation energy as a function of slab thickness. The plot indicates that the defect energies were converged within an error of 0.02 eV for slabs thicknesses greater than 20 Å. We note that the geometric thresholds for the convergence of defect energies will vary strongly with different materials. Indeed, as our results here show the geometric thresholds vary strongly between different surfaces of the same material. The high dielectric response of rutile MnO<sub>2</sub> has meant that we are able to converge our calculations explicitly to the dilute limit, but this will not be possible for all systems.

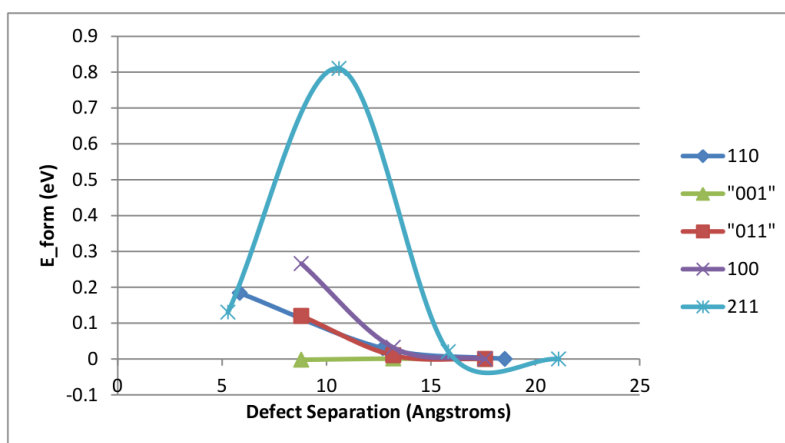


Figure S3: Calculated defect formation energies as a function of separation between a defect and its nearest periodic image in the surface plane. The zero reference formation energy is set to that calculated for the greatest separation between defects for each surface.

## References

- (1) Catlow, C. R. A. Ed. , *Computer Modelling in Inorganic Crystallography* (Academic Press, San Diego, 1997).
- (2) Hill, J. R. and Freeman, C. M. and Subramanian, L. In , *Reviews in Computational Chemistry* (Liphowitz, K. B. and Boyd , D. B. Eds., Wiley, New York, 2000).
- (3) Maphanga, R. R.; Sayle, D. C.; Sayle, T. X. T.; Ngoepe, P. E. *Phys. Chem. Chem. Phys.* **2011**, *13*, 1307.



Figure S4: Calculated defect formation energies as a function of slab thickness. The zero reference formation energy is set to that calculated for the greatest slab thickness used for each surface.

- (4) Maphanga, R.; Parker, S.; Ngoepe, P. *Surface Science* **2009**, *603*, 3184 – 3190.
- (5) Ohama, N.; Hamaguchi, Y. *Journal of the Physical Society of Japan* **1971**, *30*, 1311–1318.
- (6) Sato, H.; Enoki, T.; Isobe, M.; Ueda, Y. *Phys. Rev. B* **2000**, *61*, 3563.
- (7) Franchini, C.; Podloucky, R.; Paier, J.; Marsman, M.; Kresse, G. *Phys. Rev. B* **2007**, *75*, 195128.
- (8) Dudarev, S. L.; Botton, G. A.; Savrasov, S. Y.; Humphreys, C. J.; Sutton, A. P. *Phys. Rev. B* **1998**, *57*, 1505.
- (9) Tompsett, D. A.; Middlemiss, D. S.; Islam, M. S. *Phys. Rev. B* **2012**, *86*, 205126.
- (10) Ylvisaker, E. R.; Pickett, W. E.; Koepf, K. *Phys. Rev. B* **2009**, *79*, 035103.
- (11) Madsen, G.; Novak, P. *Europhys. Lett.* **2005**, *69*, 777.
- (12) Wang, L.; Zhou, F.; Meng, Y. S.; Ceder, G. *Physical Review B* **2007**, *76*, 165435.
- (13) Anisimov, V. I.; Zaanen, J.; Andersen, O. K. *Phys. Rev. B* **1991**, *44*, 943.
- (14) Antonides, E.; Janse, E. C.; Sawatzky, G. A. *Phys. Rev. B* **1977**, *15*, 1669.

Table S2: Predicted surface energies for  $\beta$ -MnO<sub>2</sub> from our interatomic potential model. The subscripts after the miller indices of a single surface indicate different surface terminations.

Miller Index	$E_{\text{surf}}$ (Jm <sup>-2</sup> )	Termination
(001)	2.73	MnO
(100)	2.42	O
(101) <sub>a</sub>	2.15	O
(101) <sub>b</sub>	3.92	Mn
(110) <sub>a</sub>	2.07	O
(110) <sub>b</sub>	2.88	O
(111) <sub>a</sub>	3.02	MnO
(111) <sub>b</sub>	3.32	O
(102)	3.35	O
(120) <sub>a</sub>	2.99	O
(120) <sub>b</sub>	4.11	MnO
(211) <sub>a</sub>	2.47	O
(211) <sub>b</sub>	3.22	Mn
(221) <sub>a</sub>	3.71	O
(221) <sub>b</sub>	2.33	MnO
(122) <sub>a</sub>	2.74	Mn
(122) <sub>b</sub>	2.87	Mn
(201) <sub>a</sub>	2.61	O
(201) <sub>b</sub>	2.61	O
(213) <sub>a</sub>	2.46	O
(213) <sub>b</sub>	2.50	MnO
(310) <sub>a</sub>	2.47	O
(310) <sub>b</sub>	4.01	Mn
(331) <sub>a</sub>	3.40	O
(331) <sub>b</sub>	2.28	MnO
(321) <sub>a</sub>	2.43	O
(321) <sub>b</sub>	2.74	Mn
(103) <sub>a</sub>	2.62	O
(103) <sub>b</sub>	3.81	Mn
(133)	2.47	O
(301) <sub>a</sub>	2.66	O
(301) <sub>b</sub>	2.69	Mn
(311) <sub>a</sub>	2.56	O
(311) <sub>b</sub>	2.67	O
(312)	2.44	O
(322) <sub>a</sub>	3.22	O
(322) <sub>b</sub>	2.86	MnO
(331) <sub>a</sub>	2.28	O
(331) <sub>b</sub>	3.40	MnO
(332)	2.63	O